SCIENTIFIC STUDY & RESEARCH ♦ Vol. IX (2) ♦ 2007 ♦ ISSN 1582-540X

THE ENERGY EFFICIENCY OF DIFFERENT PHOTOELECTRODES IN A PHOTOELECTROCHEMICAL CELL (PECC)♦

Alexandru I. Enesca*, Anca Duta

Research Center: Product Design for Sustainable Development, Transilvania University, Eroilor 29, 500036, Braşov, Romania

*Corresponding author: aenesca@unitbv.ro

Received: 16/05/2008
Accepted after revision: 27/06/2008

Abstract: Hydrogen production via water photolysis represents a topic very much addressed to considering the output – the cleanest fuel – and the problems to be solved, mainly the conversion efficiency. The latest is strongly linked with the photoanod material properties and represents an advanced application of thin films of wide band gap semiconductors. The paper presents a study concerning the energy efficiency of different photoelectrodes used hydrogen production in a photoelectrochemicall cell (PECC). The morphological, electrical and optoelectrical analysis were done considering the influence of bulk and surface composition on the photoelectrolysis process. The contribution of the crystalline structure, morphology and dopants is discussed in terms of optical efficiency for films obtained using an up-scalable technique: spray pyrolysis deposition. The influence of the deposition parameters is also considered correlated with the optimized values.

♦ Paper presented at the fifth edition of: "Colloque Franco-Roumain de Chimie Appliquée – COFrRoCA 2008", 25 – 29 June 2008, Bacău, Romania.

Keywords: *photoelectrolysis, photoelectrodes, optoelectrical properties, WO_3, TiO_2*

INTRODUCTION

The first encouraging signal in hydrogen production is called "Honda-Fujishima effect". This effect described the decomposition of water in hydrogen and oxygen in a photoelectrochemical cell containing a titanium dioxide electrode and a platinum electrode. This type of electrochemical cell has been subsequently replaced by a particular system for the photocatalytic water cleavage using TiO_2 powder [1 – 3].
Photovoltaic industry has developed the multi-junction cell technology that is used for photoelectrochemical (PEC) light harvesting systems that generate sufficient voltage to split water and are stable in a water/electrolyte environment. Theoretical efficiency for tandem junction systems is 42%; practical systems could achieve 18 – 24% efficiency; low-cost multi-junction amorphous silicon (a-Si) systems could achieve 7 – 12% efficiency. Not only does it eliminate most of the costs of the electrolyzer, but it also has the possibility of increasing the overall efficiency of the process [4 – 6].

EXPERIMENTAL

The FTO (F doped SnO_2 coated glass – Libbey Owens Ford TEC 20/2.5 nm) was used as a substrate for WO_3 deposition. Samples of 2 x 2 cm^2 FTO were cleaned by successive immersion in ethanol and acetone using an ultrasonic bath and dried with N_2 gas.

Precursor's preparation

Precursor preparation for undoped WO_3 films (WO_3/FTO)
The precursor $(NH_4)_2WO_4$ was obtained by mixing WO_3 powder (99.8%, Alfa Aesar) with ammonium solution (25%, J.T. Baker) at the average temperature of 60 °C, under continuous stirring, using a reflux device.

Precursor preparation for TiO_2 films (TiO_2/FTO)
The precursor was prepared using titanium(IV) isopropyl oxide, $(Ti[OCH(CH_3)_2]_4$, TTiP, 99.999%, Sigma-Aldrich) precursor, acetyl acetone, (2,4 pentadione, 99+%, $CH_3COCH_2COCH_3$, AcAc, Aldrich) as complexation and morphology control agent and absolute ethanol (C_2H_5OH, EtOH, J.T. Baker) as solvent.

Precursor preparation for WO3 films doped with Na^+ ions (WO_3_Na/FTO)
The precursor was prepared in two steps:
- 0.005 M $(NH_4)_2WO_4$ precursor was obtained in a similar way with the description made for the undoped layers;
- sodium chloride (NaCl, 99.99%, Alfa Aesar) was added as source of doping ions with 0.75 wt% atomic ratio.

Precursor preparation for TiO_2 and WO_3 wafer layers (TiO_2/WO_3/FTO)
The precursors were prepared as follows:
- $(NH_4)_2WO_4$ was obtained by mixing WO_3 powder (99.8%, Alfa Aesar) with ammonium solution (25%, J.T. Baker) at the average temperature of 60 °C under continuous stirring using a reflux device;
- titanium(IV) isopropyl oxide, ($Ti[OCH(CH_3)_2]_4$, TTiP, 99.999%, Sigma-Aldrich) precursor, acetyl acetone, (2,4 pentadione, 99+%, $CH_3COCH_2COCH_3$, AcAc, Aldrich) as complexation and morphology control agent and absolute ethanol (C_2H_5OH, EtOH, J.T. Baker) as solvent.

Precursor preparation for TiO_2 and WO_3 mixed films (WO_3-TiO_2/FTO)
The precursor was prepared using titanium chloride ($TiCl_4$, 99.999%, Alfa Aesar) and tungsten chloride (WCl_6, 99.999%, Alfa Aesar) in 1:1 molar ratio and absolute ethanol (C_2H_5OH, EtOH, J.T. Baker) as solvent.

Deposition parameters

The layers were obtained by spray pyrolysis deposition (SPD), [7, 8], using two different deposition sequence:
(1) alternating WO_3 and TiO_2 layer by layer, samples (a)-(d);
(2) one WO_3 thick layer and one TiO_2 thick layer, sample (e).
The deposition parameters are presented in Table 1, as previously optimized.

Table 1. *Deposition parameters*

Sample	SPD			
	Temperature (°C)	**Number of deposition sequences**	**Break between the deposition sequences (s)**	**Carrier gas pressure (bar)**
(a) WO_3/FTO	350	20	60	1.5
(b) TiO_2/FTO	400	20	60	1
(c) WO_3_Na/FTO	350	20	60	1.5
(d) WO_3_TiO_2/FTO	400	30	60	1.5
(e) TiO_2/WO_3/FTO	400/350	20/20	80	1.3

The doped samples were obtained according to the layer-by-layer or bulk deposition.
As post deposition process the annealing treatment was used at 500 °C, 5 h for all five samples.

Films characterization

The XRD analysis was performed using Bruker D8 Advance Diffractometer.
The morphology of the nanocomposite structure is studied using a Scanning Electron Microscope (SEM, Jeol JSM-5800LV).
For the current-voltage and photocurrent measurements (the current - voltage curves in dark) was used a DC Source Meter (Keithley, model 2400) and a HF Frequency Analyser (Solartron Schlumberger, model 1255).

RESULTS AND DISCUSSIONS

Crystallinity and morphology

The diffraction analysis (Figure 1) shows the formation of monoclinic WO_3 and TiO_2 anatase. In the Na^{+1} doped WO_3 sample comparing with the undoped sample, there are no extra-peaks that can be attributed to sodium oxide or other mixed compounds, proving that the thin films deposition conditions allowed the growth of doped tungsten oxide in similar condition with the undoped sample. The doping process corresponds to the following solid state reactions:

$$WO_3 \xrightarrow{Ta_2O_5} Ta_w^{'} + Ta_i^{\cdots\cdot} + 2O_i^{''} + O_o^{x} \quad (1)$$

$$2WO_3 \xrightarrow{Ta_2O_5} 2Ta_w^{'} + V_o^{\cdot\cdot} + 5O_o^{x} \quad (2)$$

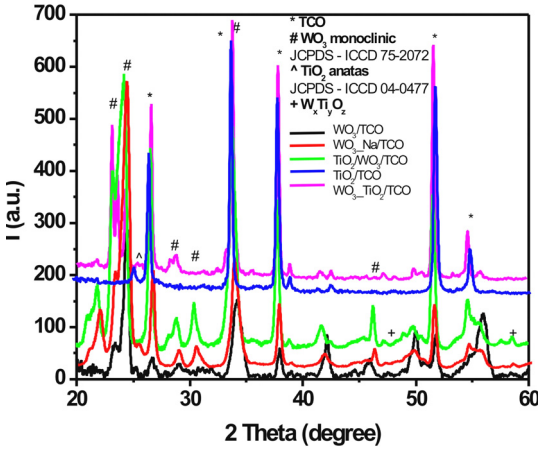

Figure 1. *Diffraction analysis of the photoelectrodes*

The most likely process is described by reaction 2, involving only two types of defects, that requires the lowest energy formation (in terms of charge and mobility). Oxygen vacancies are one of the most common defects; parts of them are passivated during the annealing process, decreasing the ionic conduction but increasing the electronic conduction:

$$V^{\cdot\cdot}{}_O + 1/2O_2 \longrightarrow O_o^{x} + 2e^{'} \quad (3)$$

The diffractograms corresponding to the samples WO_3-TiO_2/FTO and TiO_2/WO_3/FTO show the formation of both oxides, in the last case it was also identified the presence of a new peak that has not been surely identified. The new peak, at $2\theta = 37.7°$, can be attributed to an oxide containing both W^{6+} and Ti^{4+}.

The samples exhibit a porous morphology (Figure 2) favorable for interface process, like photoelectrolysis, with an average grain size between 200 nm for WO_3 and 150 nm for TiO_2 and average roughness as presented in Table 2.

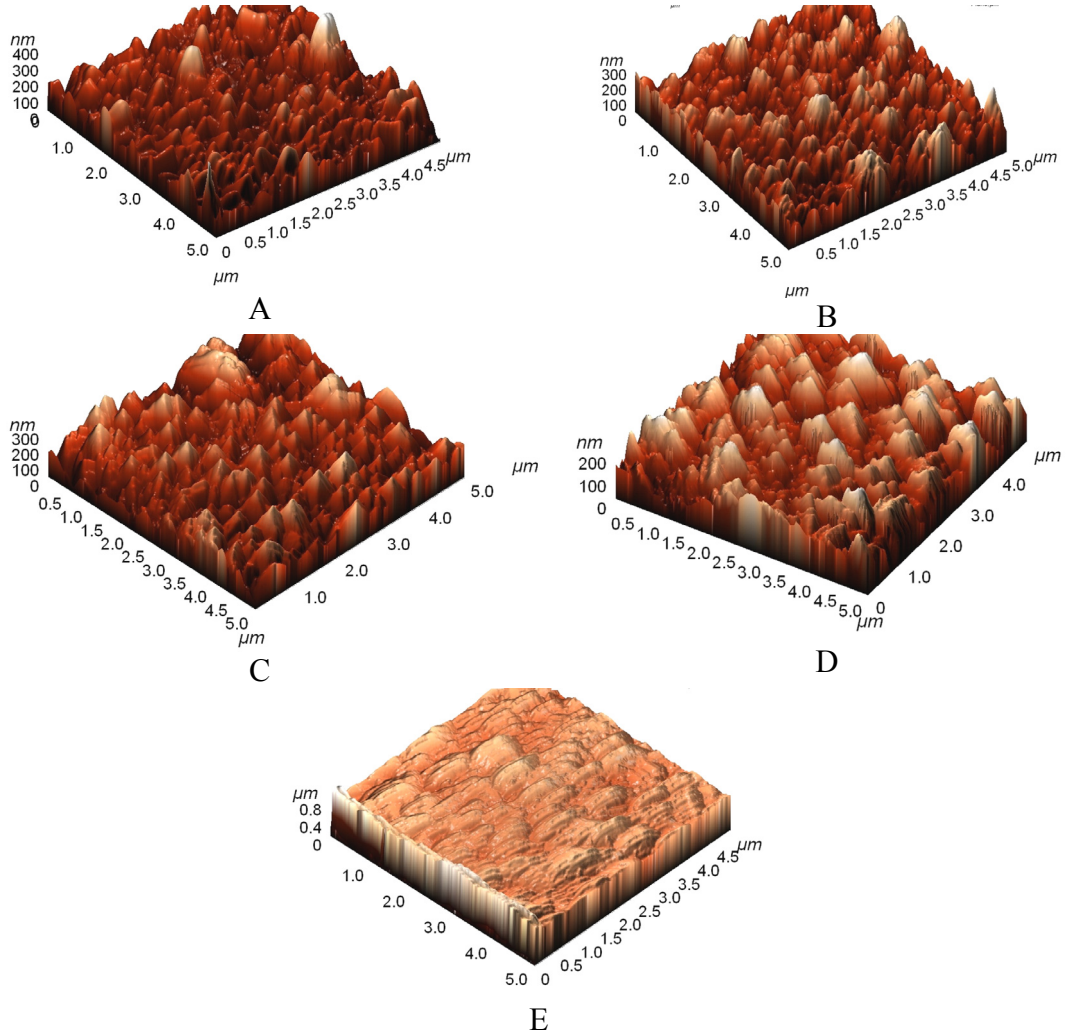

Figure 2. *AFM analysis of: (A) WO_3/FTO, (B) TiO_2/FTO, (C) WO_3_Na/FTO, (D) TiO_2/WO_3/FTO, (E) WO_3-TiO_2/FTO*

The films are homogeneous and uniform without cracks or other morphological imperfections. Major morphology changes were observed for mixed layers indicating that precursor composition and deposition steps have an important influence on the geometry of the film surface.

Table 2. *Photoelectrodes roughness*

Sample	Roughness (nm)
WO_3/TCO	150
TiO_2/TCO	100
WO_3_Na/TCO	150
TiO_2/WO_3/TCO	100
WO_3-TiO_2/TCO	100

The photocurrent analysis (Figure 3) represents one of the most representative measurements that can be done to establish the photoelectrode efficiency. Considering

that at 0V bias the sample don't show any photosensitive response, the photocurrent measurements were done at 0.5 V bias.
The higher photocurrent values were obtained for the samples TiO_2/FTO and WO_3-TiO_2/FTO even if at the beginning of light irradiation concurrent processes like electron-hole recombination or charge trapping are present.

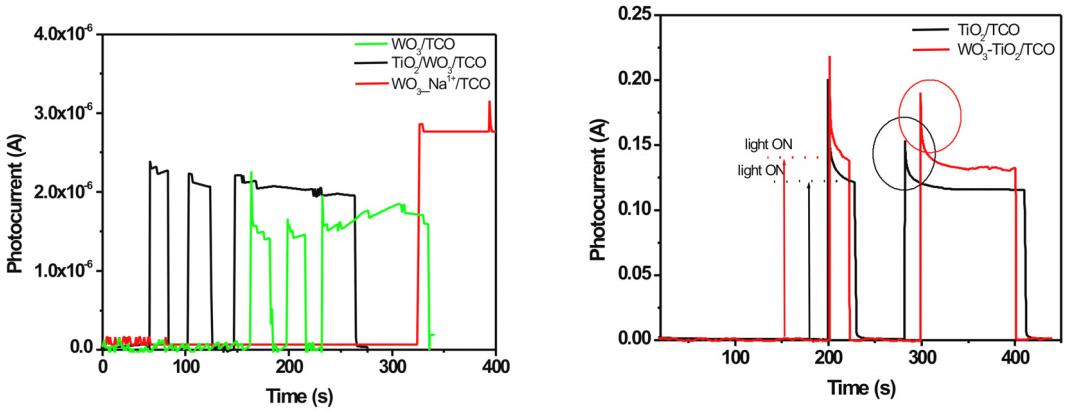

Figure 3. *Photocurrent measurements on the photoelectrochemical cell*

The samples WO_3/FTO, WO_3_Na/FTO and WO_3/TiO_2/FTO present a lower photocurrent value but are more electrically stable having a fast response (1 s) during the illumination.
The energetic efficiency diagram (Figure 4) was obtained considering the stable photocurrent value obtained for each sample during the light irradiation.

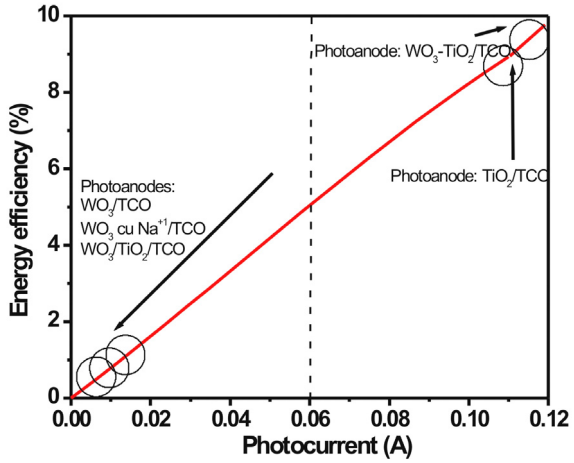

Figure 4. *Photoanodes energy efficiency*

The sample WO_3-TiO_2/FTO have the higher energy efficiency considering association of two semiconductors with comparable band gaps and with conduction and valence bands suitably disposed, can lead to a simultaneous electron transfer between the coupled semiconductors. This characteristic depends on the intimate contact between the semiconductors.

CONCLUSIONS

Five photoelectrodes containing WO_3 and TiO_2 were prepared using spray pyrolysis deposition and annealed at 500 °C. The XRD measurements prove the formation of crystalline structure with monoclinic WO_3 and TiO_2 anatase. The samples containing WO_3 exhibit a porous morphology and the sample with TiO_2 contains crystals with fractal shape. Accordingly with the photocurrents measurements the sample WO_3_TiO_2/FTO presents the higher energy efficiency as photoanode in a photoelectrochemical cell.

REFERENCES

1. Ashokkumar, M.: WO_3 Thin Films, *Hydrogen Energy*, **1998**, **23**(6), 427-438;
2. Shangguan, W., Yoshida, A., Chen, M.: Physicochemical Properties and Photocatalytic Hydrogen Evolution of TiO_2 Films Prepared by Sol-Gel Processes, *Solar Energy Materials and Solar Cell*, **2003**, **80**, 433-441;
3. Mills, A., McFarlane, M.: Current and possible future methods of assessing the activities of photocatalyst films, *Catalysis Today*, **2007**, **129**, 22-28;
4. Seyler, M., Stoewe, K., Maier, W.F.: New hydrogen-producing photocatalysts – A combinatorial search, *Applied Catalysis B: Environmental*, **2007**, **76**, 146-157;
5. Zhu, L., Chen, Y., Wu, Y., Li, X., Tang, H.: A surface-fluorinated-TiO_2-$KMnO_4$ photocatalytic system for determination of chemical oxygen demand, *Analytica Chimica Acta*, **2006**, **571**, 242-247;
6. Huang, T., Lin, X., Xing, J., Wang, W., Shan, Z., Huang, F.: Photocatalytic activities of hetero-junction semiconductors WO_3/$SrNb_2O_6$, *Materials Science and Engineering B*, **2007**, **141**, 49-54;
7. Enesca, A., Duta, A., Schoonman, J.: Study of photoactivity of tungsten trioxide (WO_3) for water splitting, *Thin Solid Films*, **2007**, **515**, 6371-6374;
8. Enesca, A., Enache, C., Duta, A., Schoonman, J.: High crystalline tungsten trioxide thin layer obtained by SPD technique, *Journal of the European Ceramic Society*, **2006**, **26**, 571-576.